Effect of interjunction coupling on superconducting current and charge correlations in intrinsic Josephson junctions

Yu. M. Shukrinov,[1] M. Hamdipour,[1,2] and M. R. Kolahchi[2]
[1]*BLTP, JINR, Dubna, Moscow Region 141980, Russia*
[2]*Institute for Advanced Studies in Basic Sciences, P.O. Box 45195-1159, Zanjan 45195, Iran*
(Received 16 April 2009; revised manuscript received 1 June 2009; published 15 July 2009)

Charge formations on superconducting layers and creation of the longitudinal plasma wave in the stack of intrinsic Josephson junctions change crucially the superconducting current through the stack. Investigation of the correlations of superconducting currents in neighboring Josephson junctions and the charge correlations in neighboring superconducting layers allows us to predict the additional features in the current-voltage characteristics. The charge autocorrelation functions clearly demonstrate the difference between harmonic and chaotic behavior in the breakpoint region. Use of the correlation functions gives us a powerful method for the analysis of the current-voltage characteristics of coupled Josephson junctions.

DOI: 10.1103/PhysRevB.80.014512 PACS number(s): 74.50.+r, 74.20.De, 74.25.Fy, 74.81.Fa

I. INTRODUCTION

The resistively and capacitively shunted junction (RCSJ) model and its different modifications are well known to describe the properties of single Josephson junctions, giving a clear picture of the role of quasiparticle and superconducting currents in the formation of current-voltage characteristics (CVC).[1–3] In the case of a stack of intrinsic Josephson junctions (IJJ) the situation is cardinally different. The system of the coupled Josephson junctions has a multiple branch structure and it has additional characteristics: the breakpoint current, the transition current to another branch, and the breakpoint region (BPR) width.[4–6] It was demonstrated that the CVC of the stack exhibits a fine structure in the BPR.[7] The breakpoint features were predicted theoretically and observed experimentally recently.[8] The breakpoint manifests itself in the numerical simulations of the other authors as well.[9]

The IJJ have a wide interest today also due to the observed powerful coherent radiation from the stack of IJJ.[10] In Ref. 11 of the manuscript, the authors summarized the experimental results and stressed that the strong emission was observed near the unstable point of the retrapping current in the uniform voltage branch when the bias current was decreased below the critical current I_c. The emission was also observed in the other branches when the bias current is further decreased below the transition points to lower branches. The radiation is related to the same region in the CVC where the breakpoint and the BPR were observed.[4–6] The breakpoints on the outermost branch and on the other branches are the unstable points, brought about by the parametric instability. So, the phase-dynamics investigation of IJJ in these CVC regions is also interesting in the context of coherent radiation emission.

The breakpoint current characterizes the resonance point, at which the longitudinal plasma wave (LPW) is created in stacks with a given number and distribution of the rotating and oscillating IJJ. These notions should be taken into account to have a correct interpretation of the experimental results. The investigation of the coupled system of Josephson junctions with a small value of the coupling parameter (as in the case of capacitive coupling), allowed us to understand in a significant way, the influence of the coupling between junctions on physical properties of the system. The capacitive coupling is realized in nanojunctions if the length of the junctions is comparable to or smaller than the Josephson penetration depth. Coupling between intrinsic Josephson junctions leads to the interesting features which are absent in single Josephson junction. The problem is complex enough for the experimental study and many questions concerning the effect of interjunction coupling on CVC are open until now. Still, the superconducting current in the coupled system of Josephson junctions with LPW has not been investigated in detail; this includes the role of the correlations of the superconducting currents in different junctions and the charge correlations on superconducting layers. In this paper we investigate these questions.

We study the phase dynamics of an IJJ stack in high-T_c superconductors. The CVC of IJJ are numerically calculated in the framework of capacitively coupled Josephson junctions model with diffusion current.[12,13] We find that the behavior of the superconducting current in the coupled system of Josephson junctions is essentially different from that of a single Josephson junction. It is demonstrated that superconducting current in the stack of IJJ reflects the main features of the breakpoint region; in particular, the fine structure in the CVC. We study various correlation functions in the characteristics, and observe that the correlations among the charge on different superconducting layers and correlations in the superconducting currents of different junctions lead to the detailed features of CVC in the BPR, and also provides additional information about the phase dynamics in the IJJ.

II. METHOD OF CALCULATIONS

To find the CVC of the stack with N IJJ, we solve a system of N dynamical equations for the gauge-invariant phase differences $\varphi_l(t) \equiv \varphi_{l,l+1}(t) = \theta_{l+1}(t) - \theta_l(t) - \frac{2e}{\hbar c}\int_l^{l+1} dz A_z(z,t)$ between superconducting layers (S layers), where θ_l is the phase of the order parameter in the S layer l, and A_z is the vector potential in the barrier. In

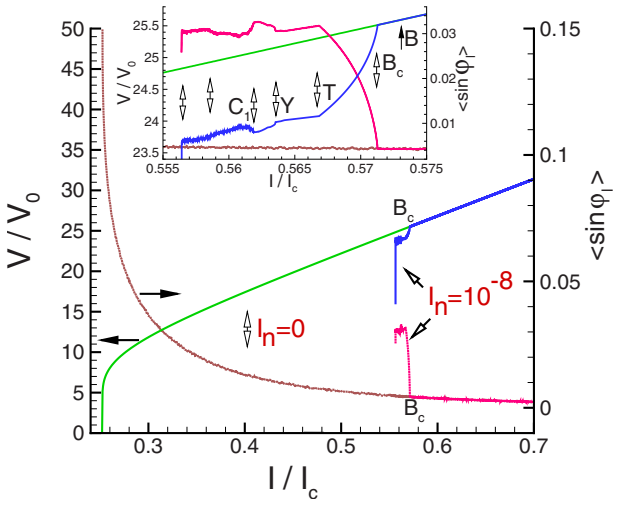

FIG. 1. (Color online) The CVC and time-averaged superconducting current $\langle \sin \phi_l \rangle$ with no noise in current ($I_n=0$) and with noise amplitude $I_n=10^{-8}$. The inset shows an enlarged view of the BPR.

our simulations we use a dimensionless time $\tau=t\omega_p$, where ω_p is the plasma frequency $\omega_p=\sqrt{2eI_c/\hbar C}$, I_c is the critical current, and C is the capacitance. The voltage is presented in units of $V_0=\hbar\omega_p/(2e)$, and the current in units of I_c. The system of equations has a form $\partial^2\varphi_l/\partial\tau^2=\Sigma_{l'}A_{ll'}[I-\sin\varphi_{l'}-\beta\partial\varphi_{l'}/\partial\tau]$ with matrix A given in Ref. 4, for periodic and nonperiodic boundary conditions (BC). Using Maxwell's equation $\mathrm{div}(\varepsilon E)=\rho/\varepsilon_0$, where ε and ε_0 are the dielectric constant of the insulating layers and permittivity of free space, relatively, we express the charge density Q_l (we call it just charge) in the S layer l by the voltages V_l and V_{l+1} in the neighboring insulating layers $Q_l=Q_0\alpha(V_{l+1}-V_l)$, where $Q_0=\varepsilon\varepsilon_0V_0/r_D^2$, and r_D is the Debye screening length. Solution of the system of dynamical equations for the gauge-invariant phase differences between S layers gives us the voltages V_l in all junctions in the stack and allows us to investigate the time dependence of the charge on each S layer. The time dependence of the charge consists of time and bias current variations. We solve the system of dynamical equations for phase differences at fixed value of bias current I in some time τ domain $(0,T_m)$ with a time step $\delta\tau$; we then change the bias current by the current step δI and repeat the same procedure for the current $I+\delta I$ in the new time interval $(T_m,2T_m)$. The values of the phase and its time derivative at the end of the first time interval are used as the initial conditions for the second time interval and so on. In our simulations we use $T_m=25000$, $\delta\tau=0.05$, $\delta I=10^{-5}$ and the dimensionless time t_r is recorded as $t_r=\tau+T_m(I_0-I)/\delta I$, where I_0 is an initial value of the bias current. In this paper the CVC and the time dependence of charge oscillations in the S layers are simulated at $\alpha=1$, and $\beta=0.2$, using periodic BC. Our results[4] demonstrate that using periodic BC is justified because the main features of the breakpoint region for stacks with an odd number of junctions having nonperiodic BC, coincide with those using periodic BC. In the stacks with an even number of junctions, the BPR in CVC does not appear, once the boundary conditions are periodic. Moreover, using periodic BC helps understand the physics of the system more easily. The details concerning the model and the numerical procedures have been presented before.[4,5,13]

III. SUPERCONDUCTING CURRENT AND ITS CORRELATIONS

Figure 1 shows the CVC and the time-averaged superconducting current $\langle \sin \phi_l \rangle$ without random noise in current and with noise amplitude 10^{-8} for stack with nine IJJ. Our simulations of the CVC without noise gives us the value of the return current as $I_r/I_c=0.2517$, which coinciding with the value obtained from the RCSJ model. In fact, in this model the relation between the return and critical currents for $\beta \ll 1$ has the form $I_r/I_c=4\beta/\pi$, so that at $\beta=0.2$ we get $I_r/I_c=0.2546$. The superconducting current without noise demonstrates the standard increase before transition to the zero voltage state.[3] The noise in current helps create the LPW in the stack and influences the superconducting current; the particular value of noise is not very important. The creation of the LPW in the stack of junctions changes the CVC drastically, leading to the breakpoint and breakpoint region in CVC. Inset shows the enlarged part of the Fig. 1 in the breakpoint region, where arrows indicate the coincidence of the main features of CVC and the superconducting current. In point B charges appear on the S layers. Before this point a fluctuation of the charge with value of about $10^{-8}Q_0$ is observed only. At point B the parametric resonance is started, the value of the charge on the S layers is increased sharply and LPW in the stack is created. We do not investigate here the charge appearance on the S layers by correlation functions because we should measure them with the precision $10^{-16}Q_0^2$. In this paper the precision in correlation functions was restricted by $10^{-14}Q_0^2$. The detailed study of charge nucleation and LPW in the stacks with even and odd number of IJJ has been performed in Ref. 14. The point B_c is a breakpoint on the CVC and it reflects the breakdown in the sharp increase in the charge's value.[7] If we take a sum of all equations $\ddot{\varphi}_l=(1-\alpha\nabla_l^2)(I-\beta\dot{\varphi}_l-\sin\varphi_l)$ for N IJJ and then find its average in time, we obtain the equation $V=\frac{N}{\beta}(I-\langle\sin\varphi\rangle)$. This equation clearly shows why our results; namely, the V curve and the $\langle\sin\varphi\rangle$ curve, demonstrate the same features.

To investigate the origin of the CVC features in the BPR, we study the correlations, $C^s_{j,j+1}$, of superconducting currents in the neighboring junctions j and $j+1$: $C^s_{j,j+1}=\langle\sin\varphi_j(\tau)\sin\varphi_{j+1}(\tau)\rangle=\lim_{(T_m-T_i)\to\infty}\frac{1}{(T_m-T_i)}\int_{T_i}^{T_m}\sin\varphi_j(\tau)\sin\varphi_{j+1}(\tau)d\tau$, where the brackets $\langle\rangle$ mean averaging over time, and T_i is the starting point in time domain from which we collect the data for averaging. In our simulations we take $T_i=50$. It was checked that any further increase in T_i keeps the CVC practically intact. The $C^s_{j,j+1}$ as functions of bias current I/I_c are presented in Fig. 2(a) for $j=1,\ldots,9$. All curves practically coincide in the interval starting from the breakpoint B until point B_c. Then we observe regular, but different, behavior for different j until point C_1, and then again $C^s_{j,j+1}$ is nearly the same for all j in the chaotic region. As we can see in Fig.

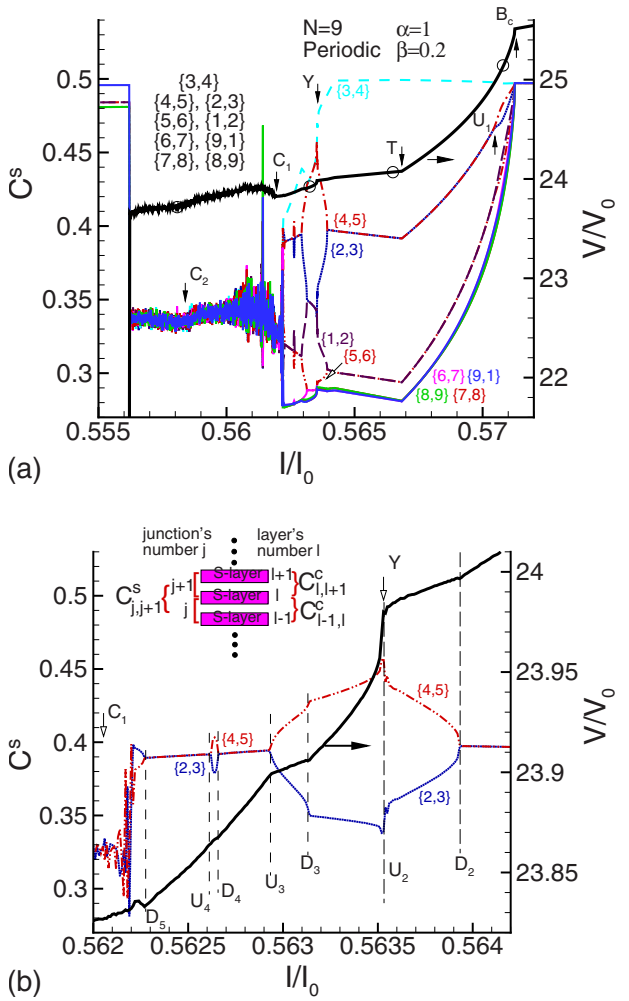

FIG. 2. (Color online) (a) The correlation of superconducting currents in the stack with nine IJJ: the curves plot the correlation functions $C^s_{j,j+1}=\langle \sin\varphi_j(\tau)\sin\varphi_{j+1}(\tau)\rangle$ as a function of bias current for all j and the thick curve shows the corresponding CVC. Labels {2 and 3}, for instance, indicates the charge or current correlations between layers 2 and 3. (b) The enlarged region in the current intervals (0.562 and 0.564). Notations for current and charge-correlation functions are also given in the inset.

2(a), eight of these functions come in pairs as $(C^s_{4,5},C^s_{2,3})$, $(C^s_{5,6},C^s_{1,2})$, $(C^s_{6,7},C^s_{9,1})$, and $(C^s_{7,8},C^s_{8,9})$; and one function, $C^s_{3,4}$ stands by itself. Let us note that because we consider a periodic BC, the number assigned to a junction is only a label. The black curve shows the outermost branch of the CVC of the stack with nine IJJ. We can see that the features of the correlation functions coincide with the features of CVC, i.e., they manifest themselves in the CVC curve. In Fig. 2(b) the part of Fig. 2(a) is plotted on an expanded scale. Thin dashed lines show the points where the features of $C^s_{j,j+1}$ coincide with those of CVC. In the inset to this figure we clarify the formation of the charge and superconducting-current correlation functions by the diagram. Study of $C^s_{j,j+1}$ allows us to find additional features in CVC when compared with the previous studies.[7] Particularly, in Fig. 2 we indicate the points D_2, D_3, D_4, and D_5 where the curves of the correlation functions diverge, and points U_1, U_2, U_3, and U_4, where they converge.

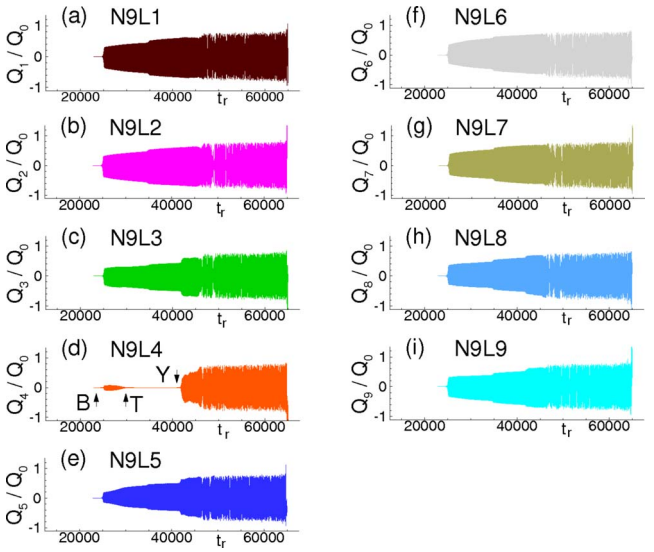

FIG. 3. (Color online) Profile of time dependence of the charge in the S layers in the stack with 9 IJJ at $\alpha=1$ and $\beta=0.2$, and with periodic BC.

IV. CHARGE CORRELATIONS AND AUTOCORRELATIONS

To understand the origin of these features, we study the time dependence of charge in the superconducting layers. In Fig. 3 we show the profiles of the charge oscillations in all layers for the stack of nine IJJ. The odd number of junctions in the stack at periodic BC leads to the case where the charge dynamics in one layer, qualitatively differs from the others; namely, the layer 4 demonstrates a specific time dependence of the charge oscillations. We will refer to this layer as the "specific layer" or the sp layer for short. The value of the charge on the sp layer is smaller than on the other layers up to point Y, and practically staying at zero, in the interval from point T until point Y. Such difference leads to the maximal value of $C^s_{3,4}$. The correlation function $C^s_{3,4}$ is different from the other correlation functions because both phase differences in it (φ_{34} and φ_{45}) are related to this unique layer. Any other correlation function has a partner which includes the same type of junction, for example, ($C^s_{4,5}$ and $C^s_{2,3}$). Figure 2(b) shows the enlarged region of Fig. 2(a) in the current interval (0.561, and 0.564). It clearly demonstrates that the features of the correlation functions reflect the features of CVC.

Let us investigate the charge correlations in the neighboring layers, using $C^c_{l,l+1}=\langle Q_l(\tau)Q_{l+1}(\tau)\rangle = \lim_{(T_m-T_i)\to\infty}\frac{1}{(T_m-T_i)}\int_{T_i}^{T_m}Q_l(\tau)Q_{l+1}(\tau)d\tau$. Here we should emphasize that the index l is a layer number. Figure 4 presents the dependence of $C^c_{l,l+1}(I/I_c)$ for different l for the stack with nine IJJ at $\alpha=1$, and $\beta=0.2$, with periodic BC. The negative sign of the $C^c_{l,l+1}$ is due to the π mode of charge oscillations so that the product of positive and negative charges gives us a negative sign for this function. Again, the correlation functions $C^c_{l,l+1}$ come in pairs: there are four pairs $(C^c_{4,5},C^c_{3,4})$, $(C^c_{5,6},C^c_{2,3})$, $(C^c_{6,7},C^c_{1,2})$, and $(C^c_{7,8},C^c_{9,1})$; here, the correlation function that stands by itself is $C^c_{8,9}$ for layers 8 and 9, which are the farthest from the sp layer (layer 4).

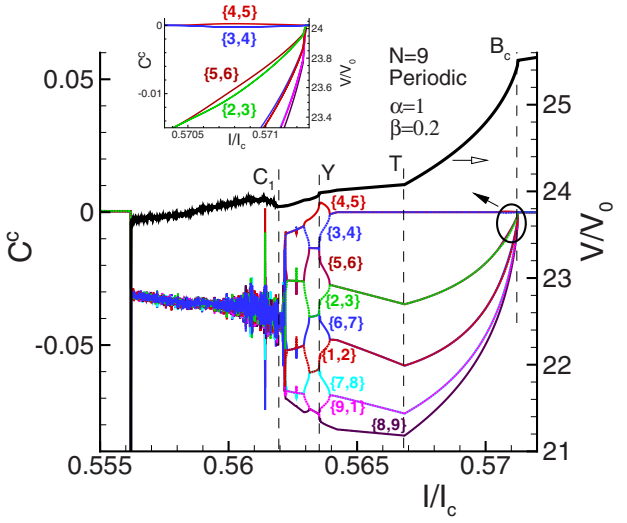

FIG. 4. (Color online) The charge correlation functions $C^c_{l,l+1}=\langle Q_l(\tau)Q_{l+1}(\tau)\rangle$ for all l in the stack with nine IJJ as a function of bias current with the thick curve showing the corresponding CVC. The inset shows the enlarged region near the point B_c.

The correlation functions ($C^c_{4,5}$ and $C^c_{3,4}$) between T and Y are close to zero because the charge on the sp layer is close to zero in this interval. The inset shows the enlarged region around point B_c, where the charge on the sp layer demonstrates its specific dynamics [see Fig. 3(d)]. The remarkable fact is that all pairs of current-correlation functions $C^s_{j,j+1}$ and charge-correlation functions $C^c_{l,l+1}$ form the loops around the point B_c in CVC reflecting the phase dynamics of the specific layer! Such loops are demonstrated clearly in Fig. 2(a) for the pairs $(C^s_{4,5}, C^s_{2,3})$ and in Fig. 4 for charge correlation functions $(C^c_{4,5}, C^c_{3,4})$ and $(C^c_{5,6}, C^c_{2,3})$. It means that the correlation functions reflect the correlations of phase dynamics among all layers and all junctions in the stack, even if the layers or junctions are far from each other. This is a demonstration of LPW in the system in other language. An interesting feature is observed in the chaotic region: At transition to the chaotic behavior (point C_1), the values of all correlation functions approach each other. The chaotic region will be discussed in detail elsewhere.

As we mentioned above, our simulation has included a random noise in the bias current. We have done the simulations at different values of the noise amplitude, from 10^{-5} to 10^{-15}. The results presented in this paper are obtained with 10^{-8}. To check for any chaotic behavior and its effects, that might be masked by this noise, on the CVC and to compare the charge oscillations in different parts of the BPR, we use the autocorrelation analysis. As is known, the autocorrelation function allows finding the repeating patterns buried under noise, or identifying the missing fundamental frequency in a signal, implied by its harmonic content. Particularly, to distinguish the harmonic oscillations in the BPR of the stack with nine IJJ, from the chaotic behavior, we study the autocorrelation of charge on the S layers

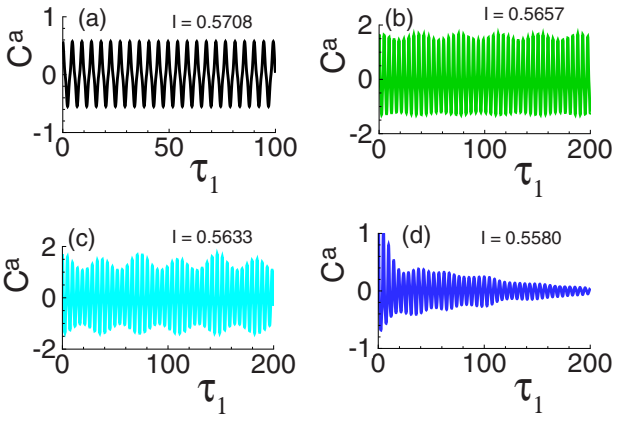

FIG. 5. (Color online) The time dependence of the autocorrelation function C^a_5 in the different parts of the BPR, marked by circles on CVC in Fig. 2(a).

by the autocorrelation function $C^a_l=\langle Q_l(\tau)Q_l(\tau-\tau_1)\rangle = \lim_{(T_m-T_i)\to\infty}\frac{1}{(T_m-T_i)}\int_{T_i}^{T_m}Q_l(\tau)Q_l(\tau-\tau_1)d\tau$. In Fig. 2(a) we show the CVC with circles at $I=0.57080$, 0.56570, 0.56330, and 0.55800, where the time dependence of the autocorrelation function $C^a_5=\langle Q_5(\tau)Q_5(\tau-\tau_1)\rangle$ is investigated. Results are presented in Figs. 5(a)–5(d). The different character of the autocorrelation function reflects the phase-dynamics features in these parts of the BPR. At $I=0.5580$, inside the chaotic domain, we can clearly distinguish the periodic motion from the chaotic one, in that C^a_5 decays to zero with increasing time τ_1.

V. SUMMARY

In summary, the phase dynamics of intrinsic Josephson junctions in the high-T_c superconductors is theoretically studied. We establish a correspondence between the features of current-voltage characteristics and the superconducting current in the breakpoint region. We investigated the superconducting current in the coupled system of Josephson junctions with LPW and clarified the role of the superconducting current correlations in different junctions, in the formation of the total CVC. We demonstrated that the correlations of the superconducting currents in neighboring junctions and the correlations of the charge on superconducting layers manifest themselves as the features on the CVC, as a consequence of the phase dynamics in the breakpoint region. We showed that the correlation analysis is a powerful tool for the investigation of the CVC of the intrinsic Josephson junctions.

ACKNOWLEDGMENTS

We thank R. Kleiner, K. Kadowaki, M. Suzuki, I. Kakeya, H. Wang, T. Hatano, and F. Mahfouzi for helpful discussions. This research was supported by the Russian Foundation for Basic Research under Grant No. 08-02-00520-a. M. Hamdipour acknowledges financial support from BLTP, JINR Dubna, Russia and IASBS, Zanjan, Iran.

[1] W. Buckel and R. Kleiner, *Superconductivity: Fundamentals and Applications* (Wiley-VCH Verlag, Weinheim, 2004).
[2] A. Barone and J. Patterno, *Physics and Applications of the Josephson Effect* (John Wiley & Sons, New York, 1982).
[3] K. K. Likharev, *Dynamics of Josephson Junctions and Circuits* (Gordon and Breach, New York, 1986).
[4] Yu. M. Shukrinov, F. Mahfouzi, and N. F. Pedersen, Phys. Rev. B **75**, 104508 (2007).
[5] Yu. M. Shukrinov and F. Mahfouzi, Phys. Rev. Lett. **98**, 157001 (2007).
[6] Yu. M. Shukrinov and F. Mahfouzi, Supercond. Sci. Technol. **20**, S38 (2007).
[7] Yu. M. Shukrinov, F. Mahfouzi, and M. Suzuki, Phys. Rev. B **78**, 134521 (2008).
[8] A. Irie, Yu. M. Shukrinov, and G. Oya, Appl. Phys. Lett. **93**, 152510 (2008).
[9] M. Machida, T. Koyama, and M. Tachiki, Phys. Rev. Lett. **83**, 4618 (1999).
[10] L. Ozyuzer *et al.*, Science **318**, 1291 (2007).
[11] T. Koyama, H. Matsumoto, M. Machida, and K. Kadowaki, Phys. Rev. B **79**, 104522 (2009).
[12] M. Machida, T. Koyama, A. Tanaka, and M. Tachiki, Physica C **330**, 85 (2000).
[13] Yu. M. Shukrinov, F. Mahfouzi, and P. Seidel, Physica C **449**, 62 (2006).
[14] Yu. M. Shukrinov and M. Hamdipour (unpublished).